Research Article

The Stability Improvement of *Aspergillus fumigatus* α-Amylase by Immobilization onto Chitin-Bentonite Hybrid

Ezra Rheinsky Tiarsa [ID],[1] **Yandri Yandri** [ID],[1] **Tati Suhartati** [ID],[1] **Heri Satria** [ID],[1] **Bambang Irawan** [ID],[2] **and Sutopo Hadi** [ID][1]

[1]*Department of Chemistry, Faculty of Mathematics and Natural Sciences, University of Lampung,*
Jl. Prof. Dr. Sumantri Brojonegoro No. 1, Bandar Lampung 35145, Indonesia
[2]*Department of Biology, Faculty of Mathematics and Natural Sciences, University of Lampung,*
Jl. Prof. Dr. Sumantri Brojonegoro No. 1, Bandar Lampung 35145, Indonesia

Correspondence should be addressed to Ezra Rheinsky Tiarsa; tiarsaezrarheinsky@gmail.com and Yandri Yandri; yandri.as@fmipa.unila.ac.id

Enzyme immobilization is a powerful method to improve the stability, reuse, and enzymatic properties of enzymes. The immobilization of the α-amylase enzyme from *Aspergillus fumigatus* on a chitin-bentonite (CB) hybrid has been studied to improve its stability. Therefore, this study aims to obtain the higher stability of α-amylase enzyme to reduce industrial costs. The procedures were performed as follows: production, isolation, partial purification, immobilization, and characterization of the free and immobilized enzymes. The CB hybrid was synthesized by bentonite, chitin, and glutaraldehyde as a cross-linker. The free enzyme was immobilized onto CB hybrid using 0.1 M phosphate buffer pH 7.5. The free and immobilized enzymes were characterized by optimum temperature, Michaelis constant (K_M), maximum velocity (V_{max}), thermal inactivation rate constant (k_i), half-life ($t_{1/2}$), and transformation of free energy because of denaturation (ΔG_i). The free enzyme has optimum temperature of 55°C, $K_M = 3.04$ mg mL^{-1} substrate, $V_{max} = 10.90\,\mu$molemL^{-1}min^{-1}, $k_i = 0.0171$ min^{-1}, $t_{1/2} = 40.53$ min, and $\Delta G_i = 104.47$ kJ mole^{-1}. Meanwhile, the immobilized enzyme has optimum temperature of 60°C, $K_M = 11.57$ mg mL^{-1} substrate, $V_{max} = 3.37\,\mu$molemL^{-1}min^{-1}, $k_i = 0.0045$ min^{-1}, $t_{1/2} = 154.00$ min, and $\Delta G_i = 108.17$ kJ mole^{-1}. After sixth cycle of reuse, the residual activity of the immobilized enzyme was 38%. The improvement in the stability of α-amylase immobilized on the CB hybrid based on the increase in half-life was four times of the free enzyme.

1. Introduction

Enzyme stability is a significant factor for commercial enzymes when applied to the batch process using a stirred-tank reactor at extreme temperature and pH*pH* [1]. Most of industrial enzymes have some problems about their thermal instability when applied in batch processes, including easily soluble in water, denatured at high temperatures, may contaminate with other substances in a reaction, and can only be used once in a process. The thermal instability of the enzyme is due to the loss of equilibrium in the noncovalent bonds [2]. Enzyme stability can be investigated by the determination of half-life and thermodynamic parameters, namely, the thermal inactivation rate constant (k_i) and the transformation of free energy because denaturation (ΔG_i) [3,4].

One of the simple methods to improve the enzyme stability, reusability, and properties is by the immobilization. After immobilization, the enzyme becomes more stable, can be easily separated from the substrate, and can be used repeatedly to the new substrate. Nowadays, immobilized enzymes have widely used on an industrial scale because of the following advantages: can be used repeatedly, the product is not contaminated by the enzyme, the reaction is

easily controlled, and can improve enzyme stability [5]. Therefore, the use of the immobilized enzymes can reduce the consumption cost. Enzyme immobilization is the process of binding or retaining enzyme molecules onto insoluble material as a supporting matrix [6] divided into organic, inorganic, and hybrid or composite material. Several methods are well known and used for enzyme immobilization such as carrier binding, encapsulation, and covalent binding [7].

The α-amylase enzyme is used as a biocatalyst to break the starch molecule down by acting on the α-1,4-glucosidic bonds to form maltose, dextrin, or D-glucose [5]. Microbial α-amylases are commonly applied in various industries such as detergent, syrup, bread and cake, dairy products, starch processing, animal feed, textile and leather, pulp and paper, candy, sugar, bioethanol, pharmaceuticals, and waste treatment [8]. This enzyme has several advantages, including an increase in production yield, decrease in production costs, controlling starch depolymerization, working at physiological conditions, preventing the formation of side products, lower energy activation, and does not need purification phase [9].

In the present study, the *Aspergillus fumigatus* α-amylase was immobilized onto a chitin-bentonite (CB) hybrid matrix. *A. fumigatus* was chosen as the host enzyme because this fungus does not show any special nutritional needs [10]. Meanwhile, chitin (poly-(β (1,4)-2-acetamide-2-deoxy-D-glucopyranose)) is a linear polysaccharide formed by N-acetyl-D-glucosamine monomer in β-linkage position [11]. Bentonite is a smectite clay mineral with two and one tetrahedral and octahedral layers [12, 13]. Chitin and bentonite were insoluble in water, has large particle surface area, chemically inert and thermally stable, easily activated, has a well-defined layered structure, has the ion-exchange ability, abundant raw material, economic, and environment friendly [11, 14]. Hybrid matrix has some benefits compared to the processes catalyzed using classic material especially for getting the better properties of the matrix and increasing thermal stability of the enzyme [7]. In the latest research, chitin-bentonite hybrid confirmed the higher adsorption capacity than the pure chitin and bentonite as an adsorbent [15]. Based on the better properties as an adsorbent, this study investigated the use of CB hybrid as a supporting matrix in the immobilization of *Aspergillus fumigatus* α-amylase by carrier binding through physical adsorption to optimize the enzyme stability improvement.

2. Materials and Methods

Local fungal isolate *A. fumigatus* was obtained from the Laboratory of Microbiology, Department of Biology, Lampung University. Meanwhile, bentonite and chitin were purchased from Sigma-Aldrich™, and all chemicals and reagents were of analytical grade.

2.1. Research Procedure. The phases of production, isolation, partial purification, and characterization of the soluble and immobilized enzymes were based on a previous study [16].

The crude enzyme was partially purified by fractionation using ammonium sulphate and dialysis [17]. The crude enzyme was partly refined by ammonium sulphate in an ice bath. The crude enzyme was brought to 0–20% saturation with ammonium sulphate. The precipitate was removed by centrifugation at 5,000 rpm for 15–20 min, and then, ammonium sulphate was added to the supernatant to 20–85% saturation [16, 17]. The precipitated protein was collected by centrifugation at 5000 rpm for 15 min at 4°C and dissolved in a minimum volume of phosphate buffer (0.025 M; pH 6.5). Then, the enzyme suspension was dialyzed in a dialysis bag (8000 Da) for 24 h at 4°C against phosphate buffer (0.01 M; pH 6.5) [16, 17]. Meanwhile, the immobilization method was based on Yandri et al. [18].

2.2. Assay of α-Amylase Activity and Determination of Protein Content. The α-amylase activity in partial purification steps was assayed by the Fuwa method using iodine reagent. The Fuwa method was used to determine the α-amylase activity based on the amount of substrate reduced for incubation time 10 min. This method was appropriate to assay the α-amylase activity in purification steps in which probably other amylases such as β-amylase and glucoamylase as an exoacting amylase [5] still exist in the crude enzyme, so that the product was specifically formed by α-amylase which breaks down the starch polymer from the middle units in rapid incubation [19]. Otherwise, the α-amylase activity in characterization steps was assayed by Mandel's method using dinitrosalicylic acid reagent. Mandel's method was used to determine the α-amylase activity based on the amount of reducing sugar (glucose) formed. This method was suitable to assay the purified enzyme which was free from other amylases [20]. In addition, the protein content was determined based on the Lowry method [21].

2.3. Chitin-Bentonite (CB) Hybrid Synthesis and Characterization. Chitin (0.5 g) was suspended into 500 mL of 1.0 M acetic acid and followed by stirring for 24 h at 30°C. Then, 5 mL of 1.0% glutaraldehyde was added as a cross-linking agent before adding 5.0 g of bentonite and stirring for 4 h at 60°C to obtain the CB hybrid. The hybrid suspension was neutralized using distilled water, and the CB hybrid was filtered and dried in an oven at 60°C. Furthermore, the dried matrix was ground by a laboratory mill and sieved [22, 23], and CB hybrid powder (0.5 g) was analyzed by FT-IR spectroscopy in the wavenumber range of 4000–650 cm^{-1} to determine the functional groups [15]. Surface morphology of the CB hybrid was characterized at 10.00 kV by scanning electron microscopy (SEM) (ZEISS).

2.4. Determination of Binding Buffer pH. The free enzyme (0.5 mL) was immobilized onto 0.2 g CB hybrid using 0.1 M phosphate buffer (0.5 mL) with the following pH variation: 6.5, 7.0, 7.5, and 8.0. Initially, these matrices (0.20 g) were washed 2-3 times using each buffer by centrifugation until pH was reached. Then, 0.5 mL of the free enzyme and 0.5 mL of each buffer were added to the matrices; then, the samples

were incubated at 4°C for 30 min and centrifuged for 15 min. About 0 25 mL of the supernatant was taken as the "binding" sample and 0.25 mL as a control, separately. Furthermore, the immobilized enzymes were eluted from each matrix using a 1.0 mL mixture of 0.1 M phosphate buffer pH 5.5 and 1 M NaCl (1 : 1), and the samples were then centrifuged for 15 min. About 0.25 mL of the supernatants was taken as the "elution" samples and assayed by the Fuwa method. Buffer pH with both of the lower enzyme activity in the binding process and the higher activity in the elution process was chosen as the binding buffer pH in the immobilization procedure.

2.5. Immobilization of α-Amylase onto CB Hybrid. CB hybrid (0.20 g) was stabilized using the binding buffer until the pH was reached, and 0.5 mL of the free enzyme and binding buffer were added to the hybrid matrix. In addition, it was incubated at 4°C for 30 min and centrifuged for 15 min. The supernatant of 0.25 mL was taken as a control, and 0.75 mL of the starch substrate was added to the immobilized enzyme. It was incubated at its optimum temperature for 30 min, and the supernatant was assayed by Mandel's method.

2.6. Determination of Optimum Temperature. Determination of optimum temperature was conducted at different incubation temperatures in Mandel's assay as follows: 50, 55, 60, 65, 70, and 75°C for 30 min. The incubation temperature, which gave the highest enzyme activity, was determined as the optimum temperature.

2.7. Steady-State Kinetics. Kinetic parameters of Michaelis constant (K_M) and the maximum velocity (V_{max}) were estimated using the Lineweaver–Burk plot from experimental data concerning the effect of the starch substrate against the enzyme activity in the following concentration range: 0.2, 0.4, 0.6, 0.8, and 1.0%. The free and immobilized enzymes were incubated at each optimum temperature for 30 min and assayed by Mandel's method. The enzyme activity is proportional to the rate of an enzyme-catalyzed reaction, and the K_M value was determined as the optimum substrate concentration [1].

2.8. Determination of Thermal Stability. Thermal stability of the enzyme was determined from the retainment of residual activity after inactivation at 60°C during the time (t_i) variations of 0, 10, 20, 30, 40, 50, 60, 70, and 80 min [24, 25]. The enzyme activity was assayed by Mandel's method, and these data were used to determine k_i, $t_{1/2}$, and ΔG_i values.

2.9. Determination of $t_{1/2}$, k_i, and ΔG_i. Determination of the thermal inactivation rate constant (k_i) and half-life ($t_{1/2}$) was calculated using the following first-order enzyme inactivation rate equation:

$$\ln\left(\frac{E_i}{E_o}\right) = -k_i \times t_i, \tag{1}$$

where k_i is the thermal inactivation rate constant, E_o is the residual activity at t_o, E_i is the residual activity at t_i, and t_i is the thermal inactivation time [4]. The slope of the graph $\ln(E_i/E_o)$ against t_i is determined as k_i.

The free energy due to denaturation (G_i) is the energy required for enzyme denaturation from the initial state. The value of ΔG_i was estimated from the following thermodynamic equation:

$$\Delta G_i = -RT \ln \frac{k_i \cdot h}{k_B \cdot T}, \tag{2}$$

where ΔG_i is the transformation of free energy because of denaturation, R is the ideal gas constant, T is the thermal inactivation temperature (K), k_i is the thermal inactivation rate constant, h is the Planck constant, and k_B is the Boltzmann constant [4].

2.10. Reusability Study. The immobilized enzyme reacted with the substrate was washed again using binding buffer by centrifugation, and 0.25 mL of the supernatant was taken as the control. Furthermore, the immobilized enzyme was reacted with a new substrate (0.75 mL) and assayed by Mandel's method.

2.11. Statistical Analysis. All measurements were done in duplicate ($n = 2$), and data were reported as mean ± standard deviation (SD). Analysis of variance (ANOVA) accompanied by the student t-test (paired two-sample for means) was conducted to identify the significant differences between two replicate samples. The level of significance was set at $p < 0.05$. The null hypothesis had been rejected, and there is no difference between the two replicate measurements.

3. Results and Discussion

3.1. Characterization of CB Hybrid. The FT-IR spectra of chitin, bentonite, and CB hybrid are shown in Figure 1. Considering the results of FT-IR, the spectrum of chitin in Figure 1(b) shows the characteristic bands at 3429.2, 3257.7–3101.1, 1625.1, 1550.6, and 1312 cm^{-1}. They are attributed to O-H stretching, N-H stretching, and amides I, II, and III, respectively. Another peak at 1013 cm^{-1} corresponded to the C-O stretching in saccharide rings [26]. In contrast, the spectrum of bentonite in Figure 1(c) shows broadband at 3623 cm^{-1} and was assigned to the O-H stretching of the silanol (Si-OH) groups coordinated to octahedral Al^{3+} cations. The HO-H vibration of the adsorbed water molecules was detected at 3406.8 cm^{-1} [27], and the sharp peak in the region of 1118–991 cm^{-1} was associated with the Si-O stretching in the tetrahedral layer [28]. The peak at 723 cm^{-1} confirmed the presence of quartz admixture [29]. On the other hand, the spectrum of CB hybrid is shown in Figure 1(a). As shown in Figure 1(a), the physical interaction between the chitin polymeric chain and
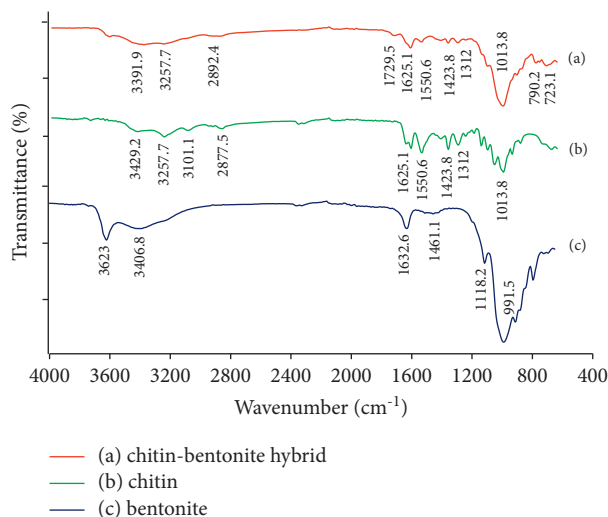
Figure 1: FT-IR spectra of chitin, bentonite, and CB hybrid materials. (a) Chitin-bentonite hybrid. (b) Chitin. (c) Bentonite.

bentonite layer cause changes in the corresponding region between 3600 and 3000 cm^{-1}. The peak at 3429 cm^{-1} corresponding to the O-H group of chitin was significantly shifted to the lower wavenumber at 3391 cm^{-1}. This band shift indicates that both the chitin and bentonite have good physical interaction through intermolecular hydrogen bonds [15]. The bands at 3101 cm^{-1} of the N-H amide groups in a chitin and 3623 cm^{-1} of the O-H group in a bentonite layer disappeared in the spectrum of CB hybrid. These results indicate the existence of good miscibility between chitin and bentonite [30], which confirmed the successful synthesis of the CB hybrid. Meanwhile, the characteristics of each matrix still exist by the existence of some functional groups.

SEM micrographs of chitin, bentonite, and CB hybrid materials are shown in Figure 2. As a result, surface morphology of CB hybrid in Figure 2(c) appeared with a significant difference compared to bentonite and chitin in Figures 2(a) and 2(b). After modification, the CB hybrid exhibits the larger pores size between the particles compared to bentonite and chitin possibly due to the intercalation of organic moiety. Based on Figure 2(c), at 9000x magnification, the CB hybrid pores size was observed about 2 μm. This leads to increase in the interlayer distance and porous aggregates formation which results in increase of the adsorption of the enzyme [31]. The intercalation of chitin expanded the bentonite basal spacing which facilitated the enzyme adsorption onto CB hybrid. The use of ratio 1 : 1 of chitin and bentonite in this study was suitable to obtain the high intensity of the bentonite basal spacing which indicates the best adsorption capacity of CB hybrid based on the previous research [15].

3.2. Determination of Binding Buffer pH.
Determination of binding buffer pH for enzyme immobilization is shown in Figure 3. The α-amylase enzyme molecules can bind onto CB hybrid through physical adsorption in the pH range of 7.0-8.0. pH 7.5 and 8.0 showed the lower enzyme activity in the binding process which indicated that the enzyme had been successfully bound onto the matrix. However, the enzyme activity at pH 8.0 in the elution process was lower than the activity at pH 7.5, in which possibly the enzyme denatured at extreme alkaline pH. In conclusion, pH 7.5 was chosen as the binding buffer pH. In the immobilization process via physical adsorption, the enzyme only can be bound onto supporting matrix at certain pH. The enzyme anionic form exists due to deprotonation of the amine group, while the OH groups in water molecules make the hybrid surface charge positive at higher solution pH [27, 32]. Since oppositely charged groups are due to the electrostatic interaction, the enzyme can be adsorbed to the positively charged active sites of the hybrid surface by the cation-exchange process [33]. At a pH range of 7.0-8.0, enzyme sorption was favored due to the electrostatic attraction between the positive surface charge of hybrid matrix and negative charge on an enzyme molecule. Therefore, the hydrogen bonding between the enzyme molecules and the hybrid matrix can be affected.

3.3. Determination of Optimum Temperature.
The temperature profiles of the free and immobilized enzymes are shown in Figure 4. The optimum temperature of the free and immobilized enzyme was 55°C and 60°C, respectively. After immobilization, the enzyme optimum temperature is shifted due to the obstruction of the space by the CB hybrid concerning the enzymatic molecules to prevent denaturation. The kinetic energy will increase with the rate of enzyme-catalyzed reaction at the optimum temperature. The active site of the enzyme will open properly to interact with the substrate after incubation at optimum temperature. Therefore, the activation energy will form the enzyme-substrate complex [34].

3.4. Steady-State Kinetics.
The Michaelis constant (K_M) and maximum velocity (V_{max}) were determined using the Lineweaver–Burk plot which describes the relationship between substrate concentration and the rate of an enzyme-
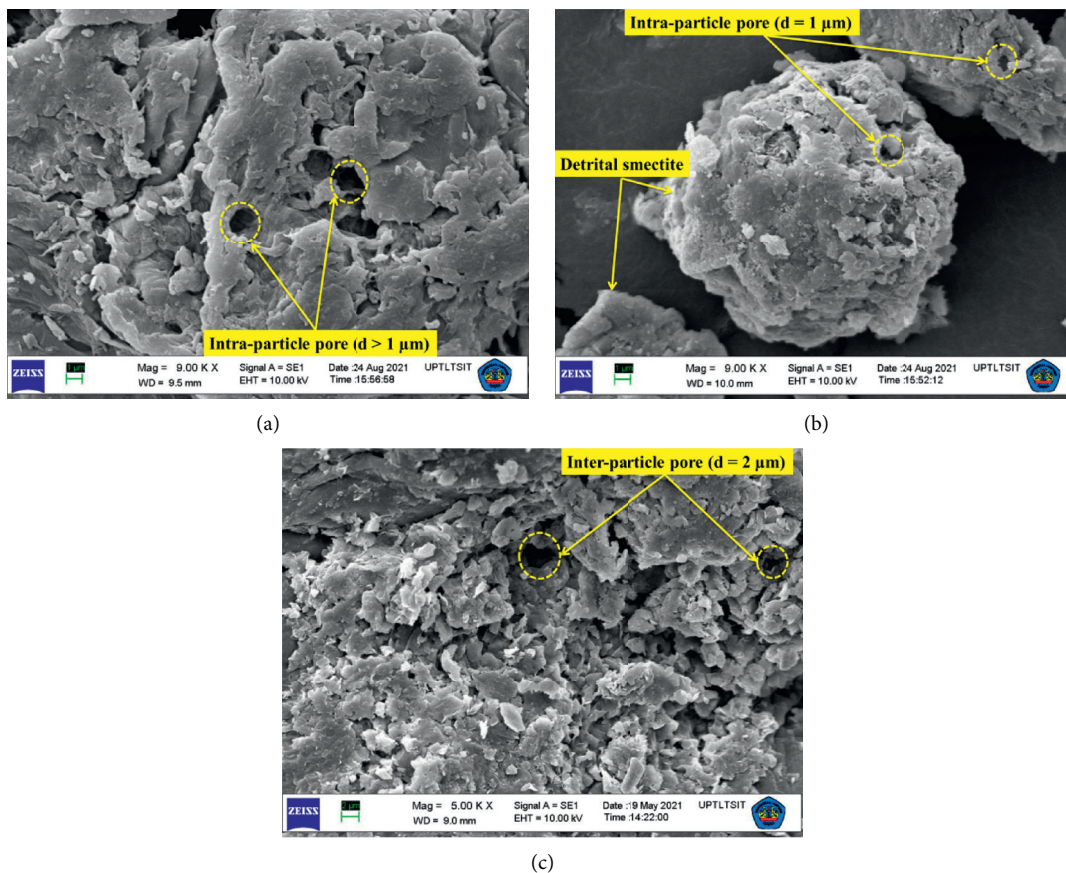
(a)

(b)

(c)

FIGURE 2: SEM micrographs of (a) chitin, (b) bentonite, and (c) CB hybrid materials.

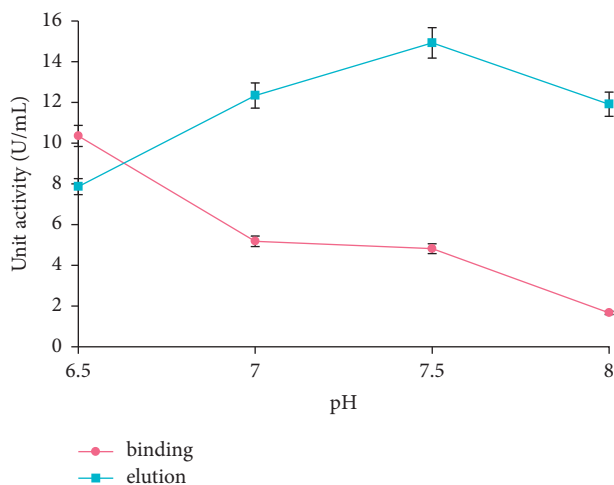FIGURE 3: Binding buffer pH for enzyme immobilization. The data are presented as mean ± SD; $n = 2$; $p \leq 0.05$. The error bars represent standard deviations from two replicates measurements.

FIGURE 4: The optimum temperature of the free and immobilized enzymes. The data are presented as mean ± SD; $n = 2$; $p \leq 0.05$. The error bars represent standard deviations from two replicates measurements.

catalyzed reaction. Meanwhile, the Lineweaver–Burk plot for free and immobilized enzymes is shown in Figure 5.

The Michaelis constant (K_M) showed the enzyme affinity for its substrate, while the maximum velocity (V_{max}) measures the extent. K_M and V_{max} values for free and immobilized enzymes are given in Table 1.
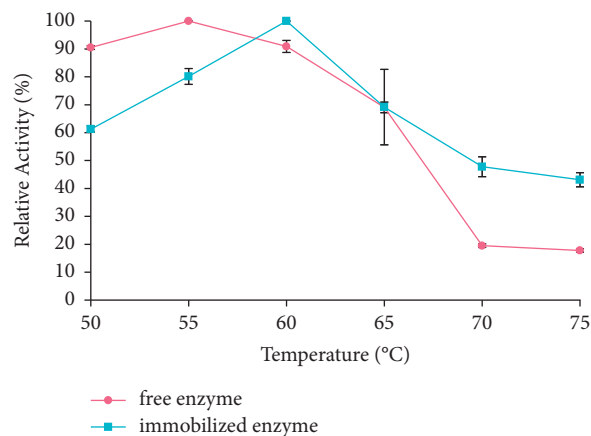
The data in Table 1 provide decreasing V_{max} and increasing K_M of the immobilized enzyme. The higher K_M of the immobilized enzyme showed a lower affinity. The change in the affinity of the immobilized enzyme due to the conformational change and the lower accessibility to the substrate reduced V_{max} of the reaction. The result indicated the
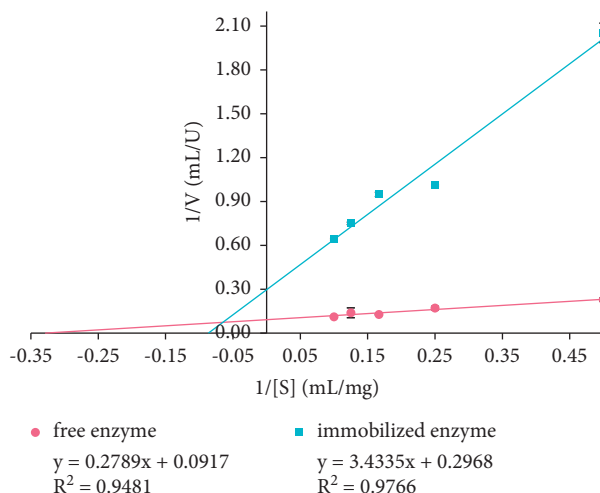
FIGURE 5: Lineweaver–Burk plot analysis of the enzymatic kinetics of free and immobilized enzyme. The data are presented as mean ± SD; $n = 2$; $p \leq 0.05$. The error bars represent standard deviations from two replicates measurements.

TABLE 1: K_M and $V_{\max}$ values for free and immobilized enzymes.

Sample	$V_{\max}$ (μmole mL^{-1} min^{-1})	K_M (mg mL^{-1} substrate)
Free enzyme	10.90 ± 1.8940	3.04 ± 1.0430
Immobilized enzyme	3.37 ± 0.1159	11.57 ± 0.7569

The kinetic parameters were determined at each optimum temperature and the starch concentrations from 2.0 to 10.0 mg/mL. The values were shown as mean ± SD, $n = 2$.
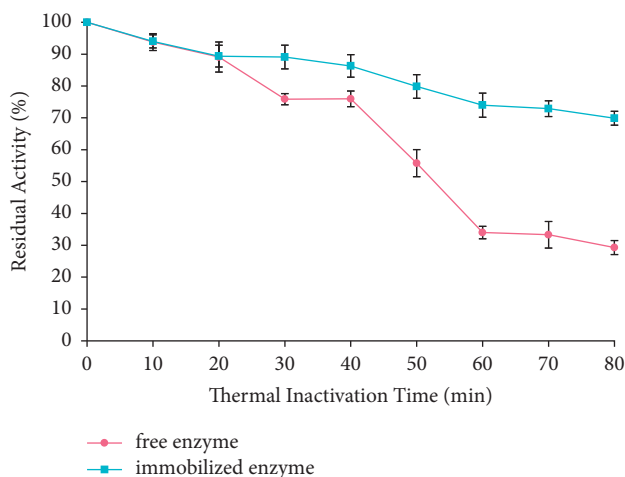

FIGURE 6: Thermal stability for free and immobilized enzymes. The data are presented as mean ± SD; $n = 2$; $p \leq 0.05$. The error bars represent standard deviations from two replicates measurements.

FIGURE 7: First-order inactivation rate plot for free and immobilized enzymes. The data are presented as mean ± SD; $n = 2$; $p \leq 0.05$. The error bars represent standard deviations from two replicates measurements.

higher substrate concentrations required to achieve maximum velocity ($V_{\max}$) [1, 35]. The immobilized enzyme showed a significant ($p < 0.05$) decrease in its reaction rate compared to the free enzyme. Therefore, the immobilized enzyme showed a significant ($p < 0.05$) increase in thermal stability compared to the free enzyme. Hybrid matrix entrapped the enzyme molecules and prevented the entrance of substrate onto the active site of the enzyme [6]. Furthe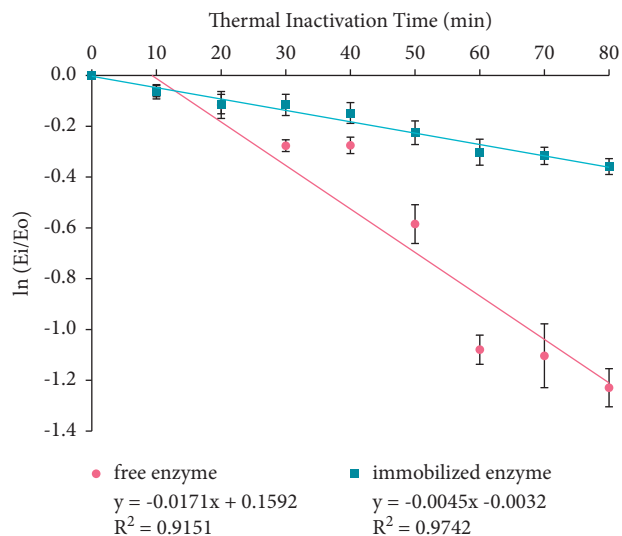rmore, the hydroxyl groups (O-H) in the hybrid surface strengthened the noncovalent bonds between the enzyme and the matrix [30].

3.5. Determination of Thermal Stability. The thermal stability for free and immobilized enzymes is shown in Figure 6. The two enzymes were thermal stable after incubation for 80 min;

TABLE 2: k_i, ΔG_i, and $t_{1/2}$ values of the free and immobilized enzymes.

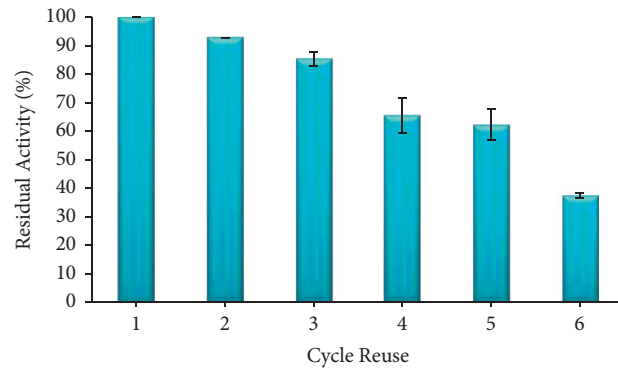| Sample	k_i (min^{-1})	$t_{1/2}$ (min)	ΔG_i (kJ mole^{-1})	Stability improvement
Free enzyme	0.0171 ± 0.0008	40.53 ± 1.9001	104.47 ± 0.1296	1
Immobilized enzyme	0.0045 ± 0.0004	154.00 ± 13.3963	108.17 ± 0.2389	3.8

The values were shown as mean $\pm$ SD, $n = 2$.

FIGURE 8: Reuse cycle of the immobilized enzyme. The data are presented as mean $\pm$ SD; $n = 2$; $p \leq 0.05$. The error bars represent standard deviations from two replicates measurements.

TABLE 3: The ratio of reuse and number of cycles for α-amylase in other experiments.

Host enzyme	Enzyme type	Matrix type	Reuse cycles	Residual activity (%)	Reference
A. fumigatus	α-Amylase	Bentonite	6	42	[16]
B. subtilis ITBCCB148	α-Amylase	Bentonite	5	43	[18]
B. subtilis	α-Amylase	Chitosan-bentonite hybrid	5	87	[22]
Saccharomyces cerevisiae	Yeast alcohol dehydrogenase	Chitin-shellac hybrid	8	46	[38]
Bovine liver	Catalase	Chitosan-bentonite hybrid	20	70	[39]
Trichoderma harzianum	α-Amylase	PPyAgNp/Fe$_3$O$_4$ nanocomposite	10	80	[40]
Thermotoga maritime	β-Glucosidase	Chitin	10	66	[41]
A. fumigatus	α-Amylase	Chitin-bentonite hybrid	6	38	This study

whereas at 60°C, the free and immobilized enzymes lost 72% and 30% of its activity, respectively. Based on the research, the immobilized enzyme molecules were protected by the matrix from the effects of extreme temperature [34]; therefore, it has higher thermal stability than the free enzyme.

3.6. Determination of $t_{1/2}$, k_i, and ΔG_i.
The residual activities for free and immobilized enzymes from thermal stability assay were plotted to the first-order enzyme inactivation rate graph as shown in Figure 7. The slope of graph $\ln(E_i/E_o)$ against t_i is expressed as a thermal inactivation rate constant (k_i). The results showed that k_i values of the free and immobilized enzymes were 0.0171 and 0.0045 min^{-1}, respectively. The thermal inactivation rate constant (k_i) was used to calculate $t_{1/2}$ and ΔG_i, as given in Table 2.

The stability improvement of the immobilized enzyme was shown in the decrease of k_i, the increase of its half-life ($t_{1/2}$), and the increase of ΔG_i compared to the free enzyme. The decrease in k_i value for immobilized enzyme showed the decrease of

denaturation rate due to the flexibility in water. Therefore, the folding conformation in the immobilized enzyme structure will increase to obtain higher stability [14]. The half-life ($t_{1/2}$) is the time required for a half inactivation of enzyme activity [4]. Based on the result, the immobilized enzyme takes a longer time to be inactivated and loses its activity; therefore, it is more stable. The immobilized enzyme has higher ΔG_i, which indicated the increase of folding conformation in tertiary structure. Furthermore, the increase in ΔG_i caused the enzyme conformation to become more rigid, stable, and less flexible in water. The energy required for enzyme denaturation becomes higher [4]. Based on the increase in half-life, the stability improvement for immobilized α-amylase enzyme onto CB hybrid was approximately four-fold higher than the free enzyme.

3.7. Reusability Study.
Immobilized enzymes can be used repeatedly on new substrates. In the enzyme immobilization through physical adsorption, the molecules cannot interact directly with the substrate [7, 36, 37]. Therefore, the enzyme

entrapped onto the matrix can be reacted to the new substrate until all molecules are exhausted. The reuse for immobilized enzyme led to a decrease in enzyme activity, and the cycle is shown in Figure 8.

As a result, the immobilized enzyme onto CB hybrid can be reused in six cycles and still retain 38% of its residual activity. The ratio of reuse and number of cycles for α-amylase in other experiments compared to this data is given in Table 3. According to the research, hybrid matrix makes biocatalyst more thermally resistant, stable under reaction conditions, the biocatalytic system becomes reusable and more efficient, improves the purity and quality of products, and protects the enzyme against conformational changes during storage, and the matrix can be more easily separated from the enzyme [7].

4. Conclusions

The stability of *A. fumigatus* α-amylase had been improved by the immobilization method onto chitin-bentonite hybrid matrix. The increase of $t_{1/2}$ and ΔG_i indicated that the immobilized enzyme become more stable and recyclable biocatalysts. Stability improvement of α-amylase enzyme by immobilization onto chitin-bentonite hybrid matrix based on increasing its half-life was approximately four-fold higher than the free enzyme. The residual activity for immobilized enzyme after sixth cycles of reuse was 38%.

Data Availability

The data used to support the findings of this study are available from the corresponding author upon request.

Conflicts of Interest

The authors declare that they have no conflicts of interest.

Acknowledgments

References

[1] P. K. Robinson, "Enzymes: principles and biotechnological applications," *Essays in Biochemistry*, vol. 59, pp. 1–41, 2015.

[2] J. Fitter, "Structural and dynamical features contributing to thermostability in α-amylases," *Cellular and Molecular Life Sciences*, vol. 62, no. 17, pp. 1925–1937, 2005.

[3] K. Ikegaya, "Kinetic analysis about the effects of neutral salts on the thermal stability of yeast alcohol dehydrogenase," *Journal of Biochemistry*, vol. 137, no. 3, pp. 349–354, 2005.

[4] D. Kazan, H. Ertan, and A. Erarslan, "Stabilization of *Escherichia coli* penicillin G acylase against thermal inactivation by cross-linking with dextran dialdehyde polymers," *Applied Microbiology and Biotechnology*, vol. 48, no. 2, pp. 191–197, 1997.

[5] A. Vogel and O. May, *Industrial Enzyme Applications*, Wiley-VCH Verlag GmbH and Co., Weinheim, Germany, 2019.

[6] M. D. Trevan, *Immobilized Enzymes, an Introduction and Application in Biotechnology*, John Wiley & Sons, New York, NY, USA, 1980.

[7] J. Zdarta, A. S. Meyer, T. Jesionowski, and M. Pinelo, "A general overview of support materials for enzyme immobilization: characteristics, properties, practical utility," *Catalyst*, vol. 8, no. 2, pp. 1–20, 2018.

[8] B. Elyasi Far, Y. Ahmadi, A. Yari Khosroshahi, and A. Dilmaghani, "Microbial alpha-amylase production: progress, challenges and perspectives," *Advanced Pharmaceutical Bulletin*, vol. 10, no. 3, pp. 350–358, 2020.

[9] M. Vitolo, "Enzymatic modification of starch," *World Journal of Pharmacy and Pharmaceutical Sciences*, vol. 9, no. 4, pp. 1341–1358, 2020.

[10] F. L. van de Veerdonk, M. S. Gresnigt, L. Romani, M. G. Netea, and J.-P. Latgé, "*Aspergillus fumigatus* morphology and dynamic host interactions," *Nature Reviews Microbiology*, vol. 15, no. 11, pp. 661–674, 2017.

[11] I. Younes and M. Rinaudo, "Chitin and chitosan preparation from marine sources. Structure, properties and applications," *Marine Drugs*, vol. 13, no. 3, pp. 1133–1174, 2015.

[12] M. Asgari and U. Sundararaj, "Silane functionalization of sodium montmorillonite nanoclay: the effect of dispersing media on intercalation and chemical grafting," *Applied Clay Science*, vol. 153, pp. 228–238, 2018.

[13] M. Ghiaci, H. Aghaei, S. Soleimanian, and M. E. Sedaghat, "Enzyme immobilization part 1. Modified bentonite as a new and efficient support for immobilization of Candida rugosa lipase," *Applied Clay Science*, vol. 43, no. 3-4, pp. 289–295, 2009.

[14] X. Y. Yang, G. Tian, N. Jiang, and B. L. Su, "Immobilization technology: a sustainable solution for biofuel cell design," *Energy & Environmental Science*, vol. 5, pp. 5540–5563, 2020.

[15] J. J. Perez, M. M. Villanuevaa, L. Sáncheze, R. Olliere, V. Alvareze, and G. J. Copelloa, "Low cost and regenerable composites based on chitin/bentonite for the adsorption potential emerging pollutants," *Applied Clay Science*, vol. 194, pp. 1–7, 2020.

[16] Y. Yandri, E. R. Tiarsa, T. Suhartati, H. Satria, B. Irawan, and S. Hadi, "The stability improvement of α-amylase enzyme from Aspergillus fumigatus by immobilization on a bentonite matrix," *Biochemistry Research International*, vol. 2022, Article ID 3797629, 7 pages, 2022.

[17] D. M. Bollag, M. D. Rozycki, and S. J. Edelstein, *Protein Methods*, John Wiley & Sons, New York, NY, USA, 2nd edition, 1996.

[18] Yandri, T. Suhartati, S. D. Yuwono, H. I. Qudus, E. R. Tiarsa, and S. Hadi, "Immobilization of α-amylase from *Bacillus subtilis* ITBCCB148 using bentonite," *Asian Journal of Microbiology, Biotechnology and Environmental Sciences*, vol. 20, no. 2, pp. 487–492, 2018.

[19] H. Fuwa, "A new method for microdetermination of amylase activity by the use of amylose as the substrate," *Journal of Biochemistry*, vol. 41, no. 5, pp. 583–603, 1954.

[20] D. E. Eveleigh, M. Mandels, R. Andreotti, and C. Roche, "Measurement of saccharifying cellulose," *Biotechnology for Biofuels*, vol. 2, no. 21, pp. 1–8, 2009.

[21] O. Lowry, N. Rosebrough, A. L. Farr, and R. Randall, "Protein measurement with the folin phenol reagent," *Journal of Biological Chemistry*, vol. 193, no. 1, pp. 265–275, 1951.

[22] Z. Baysal, Y. Bulut, M. Yavuz, and Ç. Aytekin, "Immobilization of α-amylase via adsorption onto bentonite/chitosan

composite: determination of equilibrium, kinetics, and thermodynamic parameters," *Starch-Stärke*, vol. 66, no. 5-6, pp. 484–490, 2014.

[23] Y. Gao, Y. Ru, L. Zhou, X. Wang, and J. Wang, "Preparation and characterization of chitosan-zeolite molecular sieve composite for ammonia and nitrate removal," *Advanced Composites Letters*, vol. 27, no. 5, pp. 185–192, 2018.

[24] N. E. Ahmed, A. R. El Shamy, and H. M. Awad, "Optimization and immobilization of amylase produced by *Aspergillus terreus* using pomegranate peel waste," *Bulletin of the National Research Centre*, vol. 44, no. 109, pp. 1–12, 2020.

[25] Z. Yang, M. Domach, R. Auger, F. X. Yang, and A. J. Russell, "Polyethylene glycol-induced stabilization of subtilisin," *Enzyme and Microbial Technology*, vol. 18, no. 2, pp. 82–89, 1996.

[26] E. B. Ibitoye, I. H. Lokman, M. N. M. Hezmee, Y. M. Goh, A. B. Z. Zuki, and A. A. Jimoh, "Extraction and physicochemical characterization of chitin and chitosan isolated from house cricket," *Biomedical Materials*, vol. 13, pp. 025009–025012, 2018.

[27] K. Emmerich, F. T. Madsen, and G. Kahr, "Dehydroxylation behavior of heat-treated and steam-treated homoionic cis-vacant montmorillonites," *Clays and Clay Minerals*, vol. 47, no. 5, pp. 591–604, 1999.

[28] S. Petit, "Chapter 12.6 Fourier transform infrared spectroscopy," *Developments in Clay Science*, vol. 1, pp. 909–918, 2006.

[29] P. Kumararaja, K. M. Manjaiah, S. C. Datta, and B. Sarkar, "Remediation of metal contaminated soil by aluminium pillared bentonite: synthesis, characterisation, equilibrium study and plant growth experiment," *Applied Clay Science*, vol. 137, pp. 115–122, 2017.

[30] D. Saravanan, R. Hemalatha, and P. N. Sudha, "Synthesis and characterization of cross linked chitin/bentonite polymer blend and adsorption studies of Cu (II) and Cr (VI) on chitin," *Der Pharma Chemica.*vol. 3, no. 6, pp. 406–424, 2011.

[31] M. Saeed, M. Munira, M. Nafees, A. Shah, H. Ullah, and A. Waseem, "Synthesis, characterization and applications of silylation based grafted bentonites for the removal of Sudan dyes: isothermal, kinetic and thermodynamic studies," *Microporous and Mesoporous Materials*, vol. 291, pp. 1387–1811, 2020.

[32] Y. Yandri, T. Suhartati, H. Satria, S. Karlinasari, S. D. Yuwono, and S. Hadi, "Stability enhancement of Bacillus subtilis ITBCCB148 originating α-amylase by immobilization using chitin," *Journal of Advanced Pharmacy Education & Research*, vol. 11, no. 3, pp. 63–69, 2021.

[33] A. Kumari and A. M. Kayastha, "Immobilization of soybean (Glycine max) α-amylase onto Chitosan and Amberlite MB-150 beads: optimization and characterization," *Journal of Molecular Catalysis B: Enzymatic*, vol. 69, no. 1-2, pp. 8–14, 2011.

[34] R. Fernandez-Lafuente, "Stabilization of multimeric enzymes: strategies to prevent subunit dissociation," *Enzyme and Microbial Technology*, vol. 45, no. 6-7, pp. 405–418, 2009.

[35] H. M. Abdel-Mageed, H. M. El-Laithy, L. G. Mahran, A. S. Fahmy, K. Mader, and S. A. Mohamed, "Development of novel flexible sugar ester vesicles as carrier systems for the antioxidant enzyme catalase for wound healing applications," *Process Biochemistry*, vol. 47, pp. 1152–1162, 2012.

[36] Y. Q. Almulaiky, R. M. El-Shishtawy, M. Aldhahri et al., "Amidrazone modified acrylic fabric activated with cyanuric chloride: a novel and efficient support for horseradish peroxidase immobilization and phenol removal," *International Journal of Biological Macromolecules*, vol. 140, pp. 949–958, 2019.

[37] Y. Yandri, D. Susanti, T. Suhartati, and S. Hadi, "Immobilization of α-amylase from locale bacteria isolate *Bacillus subtilis* ITBCCB148 with carboxymethyl cellulose (CM-Cellulose)," *Modern Applied Science*, vol. 6, no. 3, pp. 81–86, 2012.

[38] S. Mei, P. Han, H. Wu, J. Shi, L. Tang, and Z. Jiang, "One-pot fabrication of chitin-shellac composite microspheres for efficient enzyme immobilization," *Journal of Biotechnology*, vol. 266, pp. 1–8, 2018.

[39] J. Kaushal, S. Seema, G. Singh, and S. K. Arya, "Immobilization of catalase onto chitosan and chitosan–bentonite complex: a comparative study," *Biotechnology Reports*, vol. 18, pp. 1–7, 2018.

[40] S. A. Mohamed, M. H. Al-Harbi, Y. Q. Almulaiky et al., "Immobilization of Trichoderma harzianum α-amylase on PPyAgNp/Fe3O4-nanocomposite: chemical and physical properties," *Artificial Cells, Nanomedicine, and Biotechnology*, vol. 46, no. 2, pp. 201–206, 2018.

[41] F. Alnadari, Y. Xue, L. Zhou, Y. S. Hamed, M. Taha, and M. F. Foda, "Immobilization of β-glucosidase from thermatoga maritima on chitin-functionalized magnetic nanoparticle via a novel thermostable chitin-binding domain," *Scientific Reports*, vol. 10, no. 1663, pp. 1663–1712, 2020.